BIOCHEMISTRY
including biophysical chemistry & molecular biology

Rapid Report

pubs.acs.org/biochemistry

Simulation-Based Prediction of Phosphatidylinositol 4,5-Bisphosphate Binding to an Ion Channel

Matthias R. Schmidt,[†] Phillip J. Stansfeld,[†] Stephen J. Tucker,[‡] and Mark S. P. Sansom*,[†]

[†]Department of Biochemistry, University of Oxford, Oxford OX1 3QU, United Kingdom

[‡]Clarendon Laboratory, Department of Physics, University of Oxford, Oxford OX1 3PU, United Kingdom

Supporting Information

ABSTRACT: Protein−lipid interactions regulate many membrane protein functions. Using a multiscale approach that combines coarse-grained and atomistic molecular dynamics simulations, we have predicted the binding site for the anionic phospholipid phosphatidylinositol 4,5-bisphosphate (PIP_2) on the Kir2.2 inwardly rectifying (Kir) potassium channel. Comparison of the predicted binding site to that observed in the recent PIP_2-bound crystal structure of Kir2.2 reveals good agreement between simulation and experiment. In addition to providing insight into the mechanism by which PIP_2 binds to Kir2.2, these results help to establish the validity of this multiscale simulation approach and its future application in the examination of novel membrane protein−lipid interactions in the increasing number of high-resolution membrane protein structures that are now available.

Interactions of lipids with membrane proteins are an important component of many cell signaling pathways. The anionic lipid phosphatidylinositol 4,5-bisphosphate (PIP_2) plays a major role in such processes by acting as a secondary messenger, localizing proteins to membranes, and regulating the activity of many different classes of ion channels.[1] One of the effects of PIP_2 is the direct activation of inwardly rectifying (Kir) potassium channels that modulate cellular electrical activity, and whose dysfunction underlies a wide range of inherited channelopathies.[2,3] The binding site for PIP_2 in Kir channels was previously predicted using both conventional docking methods and simulation-based approaches.[4−6] However, these previous studies all employed homology models based upon the structure of a chimera between a eukaryotic and prokaryotic Kir channel in which several of the residues proposed to interact with PIP_2 were not fully resolved [Protein Data Bank (PDB) entry 2QKS]. Furthermore, this chimeric Kir/KirBac channel exhibits a complex functional interaction with PIP_2, and it is known that PIP_2 inhibits prokaryotic Kir channels.[7,8] Consequently, the accuracy of the binding site predicted in these original simulations remains uncertain.

In this study, we have now taken advantage of several recently determined X-ray crystal structures of eukaryotic Kir channels to evaluate the binding site for PIP_2 in the Kir2.2 channel using a multiscale molecular dynamics simulation approach.[5] This method employed coarse-grained (CG) simulations to predict initial PIP_2 binding events that were then refined by subsequent atomistic (AT) simulations.[9−13] To validate this prediction, the simulations were then compared to the crystal structures of Kir2.2 with either PIP_2 (PDB entry 3SPI) or the anionic lipid phosphatidic acid (PPA) bound (PDB entry 3SPC). An apo-state structure without any bound lipid has also been determined (PDB entry 3JYC),[14,15] and these different structures suggest an activation mechanism in which PIP_2 binding induces an upward translation and engagement of the C-terminal domain (CTD) with the transmembrane domain (TMD).[14]

To explore the influence of these different initial conformations on these predictions as well as possible effects of the lipid bilayer, bound phospholipids were removed from the 3SPI and 3SPC Kir2.2 structures, and both structures were then used as input for multiscale simulations of PIP_2 binding (Figure 1). To assess binding of PIP_2 to a Kir2.2 apo state, we also performed CG simulations using the 3JYC structure as input (Figure S1 of the Supporting Information). In addition to comparing our predicted binding sites with the PIP_2-bound 3SPI crystal structure, we also performed atomistic simulations of this PIP_2-bound structure. These reference simulations provide a more valid comparison with the multiscale simulations, because it is then possible to directly compare simulations of both proteins embedded in a phospholipid bilayer at room temperature, rather than comparing a membrane-bound simulation with a static X-ray structure in the absence of a membrane.

Examination of the 3SPI crystal structure shows that residues that make contacts with the PIP_2 headgroup (Figure 1A) are mostly basic and are located on either the N-terminal end of the first transmembrane helix TM1 (R78, W79, and R80) or the C-linker that connects the TMD with the CTD (K183, R186, K188, and K189).[14] We found that in the reference simulation of this structure all PIP_2−protein contacts were retained and accounted for nearly 90% of the total contacts made by side chains with the PIP_2 headgroups (Figure 1B). Those residues that made less frequent contacts (∼5%) with the PIP_2 headgroups (K183 and R186) were located on the C-linker. The C-linker is helical in the PIP_2-bound 3SPI structure, but flexible in other Kir2.2 crystal structures, and may therefore account for the differences observed for K183 and R186 in these simulations. However, the reference simulations appear to confirm the stability of the 3SPI structure and of the PIP_2−protein interactions in this structure.

Received: October 4, 2012
Revised: December 27, 2012
Published: December 27, 2012

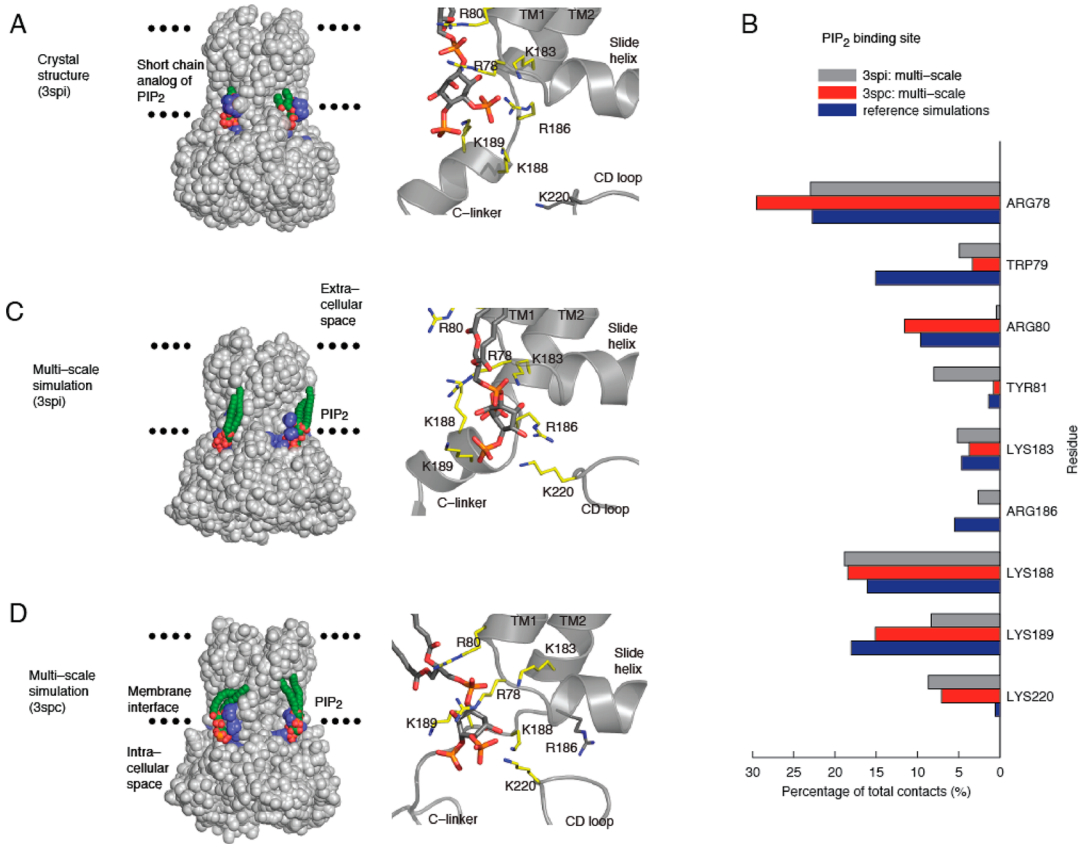

Figure 1. PIP_2 binding in Kir2.2 multiscale simulations. (A) Crystal structure with PIP_2 bound. For clarity, only two PIP_2 molecules are shown, with PIP_2-interacting residues colored blue (left). Detailed view of the PIP_2 binding site (right) as found in the 3SPI structure. (B) Multiscale simulations used either 3SPI or 3SPC as the starting structure and combined coarse-grained (CG; 24 × 0.5 μs) and atomistic (AT; 2 × 0.1 μs) simulations. Reference simulations were AT (2 × 0.1 μs) of the PIP_2-bound 3SPI crystal structure. Residues whose side chains make more than 5% of the total contacts (≤4 Å) with PIP_2 headgroups are compared between the multiscale and reference simulations. (C and D) Binding site of PIP_2 predicted by a (C) 3SPI or (D) 3SPC multiscale simulation. Parameters for PIP_2 can be found in the Supporting Information (Figure S4 and Table 1).

Importantly, we found that the multiscale simulations that used the protein coordinates from 3SPI as a starting structure predicted the PIP_2 headgroup to bind to the same cluster of basic residues as observed in the crystal structure (Figure 1C). This is in excellent agreement with both the reference simulations of this structure and earlier predictions for other Kir channels.[5,6] Residues on TM1 (R78) and on the C-linker (K183, R186, K188, and K189) were found to form the same number of contacts in the 3SPI multiscale simulations as in the reference simulations (Figure 1B). Residue W79 on TM1 formed fewer contacts in the multiscale simulations (5%) than in the reference simulations (15%). The absence of any specific hydrogen bond interactions of W79 with PIP_2 in the crystal structure is likely to render the orientation of this side chain more flexible and might be the reason for less frequent contacts between W79 and PIP_2 in the multiscale simulations compared to the reference simulations. Although W79 is suggested to facilitate PIP_2 binding by anchoring TM1 at the membrane interface,[14] less frequent contacts argue against a direct interaction of W79 with PIP_2. The two adjacent residues (R80 and Y81) also exhibit differences between the multiscale and reference simulations, but this is most likely to be related to changes in TM2 that occur during the onset of channel gating. Nevertheless, these results demonstrate agreement among the PIP_2-bound 3SPI crystal structure, the 3SPI multiscale simulations, and the reference simulations.

In addition to using 3SPI, we also used the 3SPC protein coordinates as an input for the multiscale predictions. This structure was crystallized with the anionic phospholipid PPA instead of PIP_2 and more closely resembles the apo-state structure (3JYC) in which the CTD is detached and not fully engaged with the TMD.[14] Strikingly, we found that when the ligand-free 3SPC structure was used as a starting point for the multiscale simulations of PIP_2 binding, there was also good agreement between the multiscale simulations and reference simulations (Figure 1D). Almost all contacts that were observed in the reference simulations were predicted by the 3SPC multiscale simulations (Figure 1B) and were similar to those using 3SPI as a starting structure. The only major difference was the absence of any interaction between the headgroup of PIP_2 and R186 (Figure 1B). This is probably because in the 3SPC starting structure this "C-linker" is less well ordered and the R186 side chain points in the opposite direction when compared to the PIP_2-bound 3SPI structure. Longer simulations may therefore be needed to see if R186 changes its orientation to interact with the PIP_2 headgroup.

Together, these results clearly demonstrate that the multiscale simulation approach can accurately predict the binding site for PIP_2 in Kir2.2 even when slightly different input structures are used. The principal advantage of the multiscale approach compared to conventional docking methods is that both PIP_2 and the Kir2.2 channel are flexible. This can therefore provide insights into the molecular mechanisms

dx.doi.org/10.1021/bi301350s | *Biochemistry* 2013, 52, 279−281

underlying PIP_2 binding, such as conformational changes or an electrostatic contribution (Figure S2 of the Supporting Information), which more static docking approaches lack. Interestingly, during the simulations, we observed that the phosphates of the PIP_2 headgroup formed transient hydrogen bonds with K220 on the CD loop. This resulted in a decrease in the C_α–C_α distance between K220 and a highly conserved aspartate on the slide helix (D76) of 2–4 Å. This motion appears to be due to the CD loop moving upward toward the slide helix and C-linker during PIP_2 binding, similar to the gating mechanism proposed in several other studies[16,17] and which may form part of a general activation mechanism for Kir channels by PIP_2.[6] Our results also suggest that binding of PIP_2 to the C-linker stabilizes its α-helical structure and may account for the interaction of PIP_2 with R186 in the 3SPI crystal structure. Moreover, using the multiscale approach, the effect of lipid bilayer composition on PIP_2 binding can be studied. Studies of liposomes with a controlled lipid composition highlighted an anionic secondary lipid requirement for PIP_2-induced Kir channel activation.[18] We therefore repeated our CG simulations, replacing half of the lipids on the inner leaflet with the anionic phospholipid phosphatidylserine (PS), noting that PIP_2 still binds to Kir2.2, while PS, accumulating on either side of the slide helix, is distributed unevenly around Kir2.2 (Figure S3 of the Supporting Information). This suggests a secondary binding site for anionic lipids in Kir channels.

In conclusion, these findings demonstrate good agreement among the PIP_2-bound crystal structure, the multiscale predictions, and the reference simulations and therefore validate this multiscale approach[5,6] for the prediction of PIP_2 binding sites. Consequently, this method may be confidently applied to the prediction of novel PIP_2 binding sites as well as the exploration of other lipid–channel interactions. For example, several eukaryotic voltage-gated potassium channels are regulated by PIP_2,[19,20] and enough high-resolution crystal structures now exist to allow similar multiscale simulations of binding of PIP_2 to these structures. Also, cholesterol has been shown to directly regulate Kir channel function, but its precise binding site is unknown.[21] Many other unrelated ion channels and transporters, as well other classes of membrane proteins, have also been shown to be regulated by lipids.[22−24] Therefore, this multiscale approach now provides an important and powerful tool for helping to study protein–lipid interactions and will become increasingly important with the ever-expanding number of high-resolution membrane protein crystal structures now available.

■ ASSOCIATED CONTENT

Supporting Information

Detailed methods, PIP_2 binding to an apo structure (PDB entry 3JYC), electrostatic potential mapped on the PIP_2 binding site, simulations in a mixed bilayer, and the root-mean-square fluctuations of the PIP_2 binding site. This material is available free of charge via the Internet at http://pubs.acs.org.

■ AUTHOR INFORMATION

Corresponding Author

*Phone: +44 1865 613306. E-mail: mark.sansom@bioch.ox.ac.uk.

Funding

This work was supported by the Engineering and Physical Sciences Research Council, Pfizer Neusentis, the Biotechnology and Biological Sciences Research Council, and the Wellcome Trust.

Notes

The authors declare no competing financial interests.

■ ACKNOWLEDGMENTS

We thank Dr. Prafulla Aryal for most helpful comments on the manuscript.

■ REFERENCES

(1) Suh, B. C., and Hille, B. (2008) *Annu. Rev. Biophys. 37*, 175–195.
(2) Ashcroft, F. M. (2006) *Nature 440*, 440–447.
(3) Lopes, C. M., Zhang, H., Rohacs, T., Jin, T., Yang, J., and Logothetis, D. E. (2002) *Neuron 34*, 933–944.
(4) Haider, S., Tarasov, A. I., Craig, T. J., Sansom, M. S., and Ashcroft, F. M. (2007) *EMBO J. 26*, 3749–3759.
(5) Stansfeld, P. J., Hopkinson, R., Ashcroft, F. M., and Sansom, M. S. (2009) *Biochemistry 48*, 10926–10933.
(6) Meng, X.-Y., Zhang, H.-X., Logothetis, D. E., and Cui, M. (2012) *Biophys. J. 102*, 2049–2059.
(7) Leal-Pinto, E., Gómez-Llorente, Y., Sundaram, S., Tang, Q.-Y., Ivanova-Nikolova, T., Mahajan, R., Baki, L., Zhang, Z., Chavez, J., Ubarretxena-Belandia, I., and Logothetis, D. E. (2010) *J. Biol. Chem. 285*, 39790–39800.
(8) D'Avanzo, N., Cheng, W. W. L., Doyle, D. A., and Nichols, C. G. (2010) *J. Biol. Chem. 285*, 37129–37132.
(9) Stansfeld, P. J., and Sansom, M. S. P. (2011) *J. Chem. Theory Comput. 7*, 1157–1166.
(10) Monticelli, L., Kandasamy, S. K., Periole, X., Larson, R. G., Tieleman, D. P., and Marrink, S.-J. (2008) *J. Chem. Theory Comput. 4*, 819–834.
(11) Berger, O., Edholm, O., and Jähnig, F. (1997) *Biophys. J. 72*, 2002–2013.
(12) Scott, W. R. P., Hunenberger, P. H., Tironi, I. G., Mark, A. E., Billeter, S. R., Fennen, J., Torda, A. E., Huber, T., Kruger, P., and Van Gunsteren, W. F. (1999) *J. Phys. Chem. A 103*, 3596–3607.
(13) Hess, B., Kutzner, C., Van der Spoel, D., and Lindahl, E. (2008) *J. Chem. Theory Comput. 4*, 435–447.
(14) Hansen, S. B., Tao, X., and MacKinnon, R. (2011) *Nature 477*, 495–498.
(15) Tao, X., Avalos, J. L., Chen, J., and MacKinnon, R. (2009) *Science 326*, 1668–1674.
(16) Whorton, M. R., and MacKinnon, R. (2011) *Cell 147*, 199–208.
(17) Bavro, V. N., De Zorzi, R., Schmidt, M. R., Muniz, J. R. C., Zubcevic, L., Sansom, M. S. P., Vénien-Bryan, C., and Tucker, S. J. (2012) *Nat. Struct. Mol. Biol. 19*, 158–163.
(18) Cheng, W. W. L., D'Avanzo, N., Doyle, D. A., and Nichols, C. G. (2011) *Biophys. J. 100*, 620–628.
(19) Rodriguez-Menchaca, A. A., Adney, S. K., Tang, Q.-Y., Meng, X.-Y., Rosenhouse-Dantsker, A., Cui, M., and Logothetis, D. E. (2012) *Proc. Natl. Acad. Sci. U.S.A. 109*, 2399–2408.
(20) Kruse, M., Hammond, G. R. V., and Hille, B. (2012) *J. Gen. Physiol. 140*, 189–205.
(21) Rosenhouse-Dantsker, A., Logothetis, D. E., and Levitan, I. (2011) *Biophys. J. 100*, 381–389.
(22) Tucker, S. J., and Baukrowitz, T. (2008) *J. Gen. Physiol. 131*, 431–438.
(23) Coskun, U., and Simons, K. (2011) *Structure 19*, 1543–1548.
(24) Aponte-Santamaría, C., Briones, R., Schenk, A. D., Walz, T., and De Groot, B. L. (2012) *Proc. Natl. Acad. Sci. U.S.A. 109*, 9887–9892.